Evaluating the Pharmacology and Neurotoxic Predictability of Neuroactive Compounds using Human Induced Pluripotent Stem Cell-derived Glutamatergic Neurons Co-Cultured with Astrocytes Using a Microelectrode Array Platform

Jenifer A. Bradley, Monica Metea, and Christopher J. Strock

Cyprotex US, LLC. Watertown, MA

CYPROTEX
AN EVOTEC COMPANY

Abstract

Microelectrode array (MEA) technology is recognized as a robust and reliable tool for assessing the seizurogenic and neurotoxic potential of chemical entities using rodent neuronal models. Until recently, human neuronal models lacked complex burst organization and network characteristics, which made MEA electrophysiological neurotoxic prediction challenging. Advancements in hiPSC neuronal models have addressed these limitations and provided a viable option for assessing CNS drug-induced liabilities. We have developed an early screening model for neurotoxicity using hiPSC glutamatergic neurons with astrocytes. The co-cultures were plated on 48-well MEA plates and maintained for 14-18 days, allowing formation of a robust neural network displaying complex burst organization and network (synchrony) characteristics. When this maturation process was complete, the cells were treated with different target-specific neurotoxins and seizurogenic compounds, and dose-response curves were generated. These included the proconvulsants bicuculline and picrotoxin (GABA$_A$ receptor antagonists); SNC80 (δ-opioid receptor agonist); strychnine (glycine receptor antagonist); 4-aminopyridine (potassium channel blocker); pilocarpine (cholinergic and muscarinic receptor agonist); and the neurotoxin domoic acid. Spike train analyses aligned with expected in vivo effects of these compounds and confirmed the predictability of the model. Compared to vehicle control 0.2% DMSO, 10μM domoic acid caused a complete loss in spike activity; 4-aminopyridine caused an increase in burst organization and synchrony. Strychnine caused a unique dose response pattern with changes in spike/burst rates and effects on burst and network organization while SNC80 caused a significant increase in burst activity and changes in burst structure. Pilocarpine caused a complete loss in burst organization and synchrony with a decrease in firing and burst rates.

In conclusion, hiPS cell-derived glutamatergic neurons plated with hiPSC derived astrocytes are a robust model suitable for the evaluation of potential neurotoxic and seizurogenic compounds when tested on a multi-well MEA platform.

Cellular Dynamics International's (CDI) GlutaNeurons and iCell Astrocytes

- iCell GlutaNeurons: iPS cell-derived human glutamatergic-enriched cortical neurons.
- iCell Astrocytes: iPS cell-derived human astrocytes.

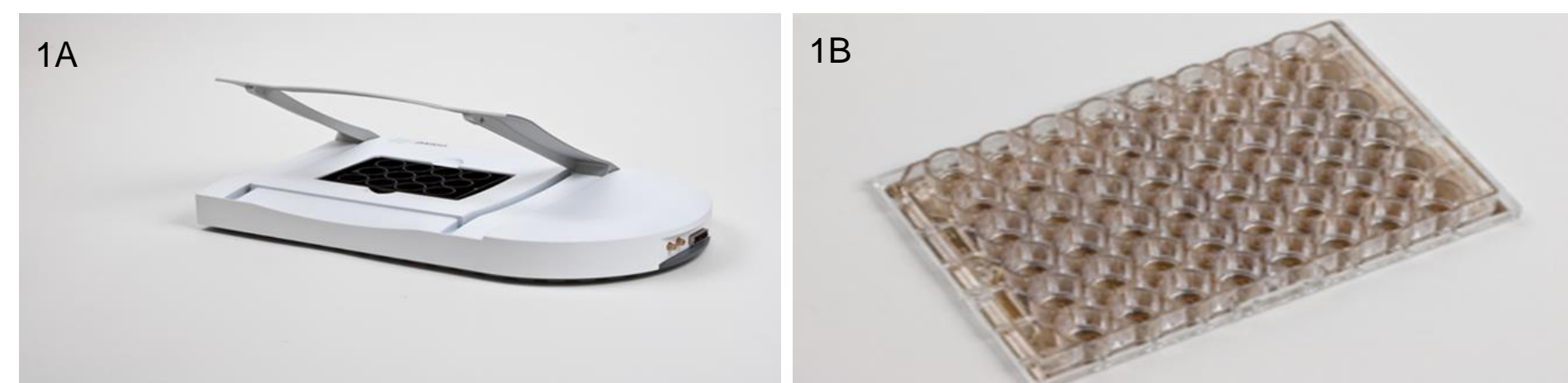## Axion BioSystems' Maestro Microelectrode Array (MEA) Platform

Figure 1A. The Maestro, Axion BioSystems. 768 recording channels with fully integrated heater and software controls. Accommodates 12, 48 and 96 well MEA plates. Figure 1B. 48 well configured MEA plate, Axion BioSystems. 16 microelectrodes per well, ANSI compliant, nano-textured gold electrodes with evaporation reducing lid.

- All recordings were acquired on the Axion Maestro platform using 48-well configured MEA plates. The Axion ECmini was used to deliver pre-mixed CO_2 throughout the recordings. A Constant temperature of 37°C was maintained through the software controller.

Methods

- 48-well MEA plates were pre-coated with a 0.07% PEI solution, rinsed and allowed to dry overnight.
- iCell GlutaNeurons and iCell Astrocytes were rapidly thawed and slowly diluted (to avoid osmotic shock) with BrainPhys Neuronal Medium supplemented with iCell DopaNeurons Supplement, iCell Nervous System Supplement, N2 supplement, Laminin and Penicillin/Streptomycin.
- After a gentle centrifugation step, the cells were resuspended at the appropriate density with cell dotting medium (complete BrainPhys Medium supplemented with additional laminin).
- A 10μL droplet of a cell suspension containing 120K iCell GlutaNeurons and 20K iCell Astrocytes was dispensed directly over the electrode grid of each well of a 48-well MEA plate.
- The cells were incubated, humidified at 37°C in 5% CO_2 for 1 hour.
- 500 μL of complete BrainPhys medium was slowly added to each well in a 2-step process to avoid detaching the cells.
- Cells were maintained for 14-18 days by changing 50% medium 3 times a week.
- Recordings were acquired on the Axion Biosystems' Maestro periodically throughout the maintenance period to document the maturation process.
- Recordings were also acquired immediately before compound treatment (baseline) and 1 hour post treatment. All experiments were performed 14-18 days after plating.
- Custom MATLAB scripts were used to analyze the spike trains. Endpoints reported include: firing rate, burst rate, number of spikes in bursts, percent isolated spikes, ISI CV, normalized IQR burst duration, burst duration, interburst interval, mean of ISI-distance, IQR/median ISI, skewness ISI, normalized MAD burst spike number, median/mean ISI and median ISI.
- Raster plots were generated with Axion BioSystems' Neural Metric Tool.

Results: Maturation
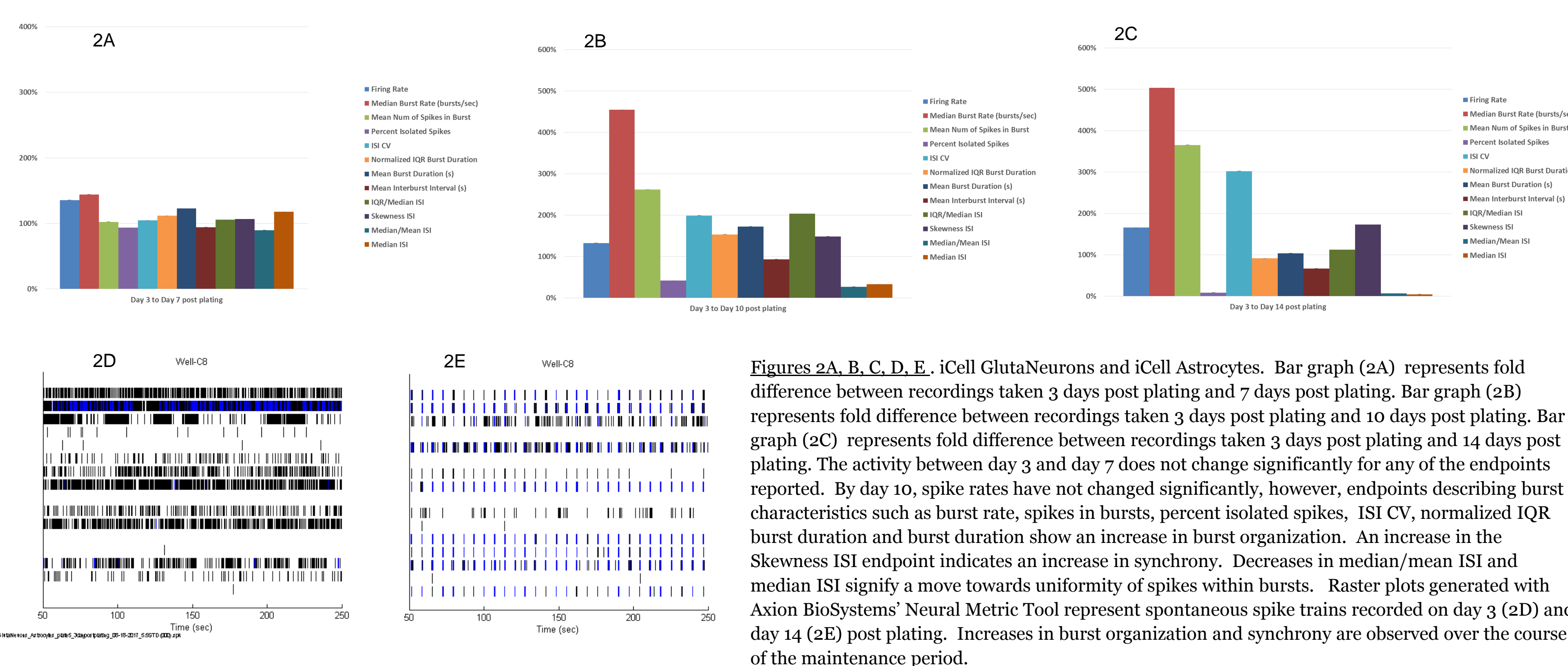
Figures 2A, B, C, D, E. iCell GlutaNeurons and iCell Astrocytes. Bar graph (2A) represents fold difference between recordings taken 3 days post plating and 7 days post plating. Bar graph (2B) represents fold difference between recordings taken 3 days post plating and 10 days post plating. Bar graph (2C) represents fold difference between recordings taken 3 days post plating and 14 days post plating. The activity between day 3 and day 7 does not change significantly for any of the endpoints reported. By day 10, spike rates have not changed significantly, however, endpoints describing burst characteristics such as burst rate, spikes in bursts, percent isolated spikes, ISI CV, normalized IQR burst duration and burst duration show an increase in burst organization. An increase in the Skewness ISI signify a move towards uniformity of spikes within bursts. Raster plots represent spontaneous spike trains recorded on day 3 (2D) and day 14 (2E) post plating. Increases in burst organization and synchrony are observed over the course of the maintenance period.
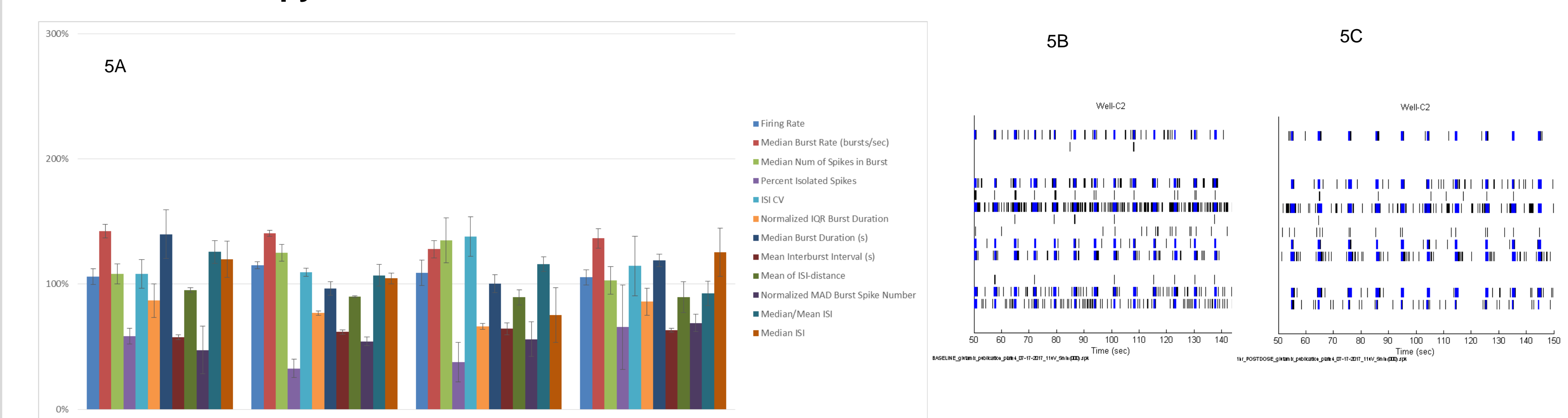
Results: Bicuculline
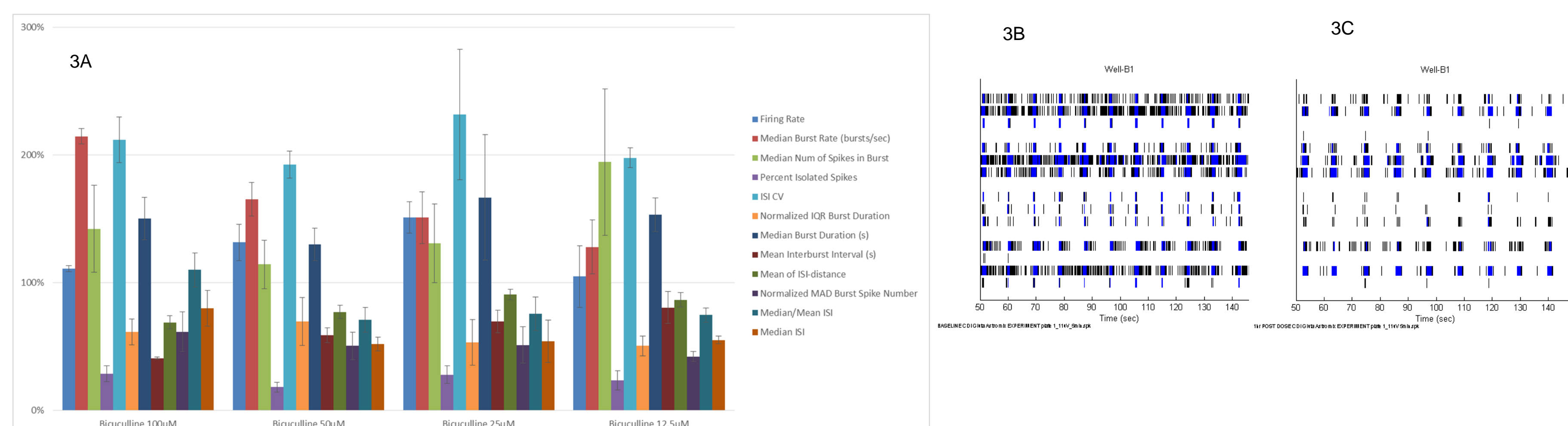
Figures 3A, B, C. Pharmacology results: Bicuculline. Bar graph (3A) represents fold difference between baseline and 1 hr post dose treatment with bicuculline at 100, 50, 25 and 12.5 μM. Results indicate significant changes in all reported endpoints. There was an overall increase in activity with an increase in both the spike rate and burst rate for all doses. Burst organization also increased after treatment indicated by an increase in the number of spikes in bursts, a decrease in the percent of isolated spikes, an increase in the ISI CV (signifies an increase in the 'burstiness' of the spike train), a decrease in the normalized IQR burst duration (signifies an increase in burst duration regularity) and an increase in the burst duration. The mean interburst interval decreased as a result of the increase in burst rate. Normalized MAD burst spike number (statistical dispersion of spikes in burst), median/mean ISI and median ISI decreased for most doses, also indicating an increase in the organization of spike train bursts. The synchrony endpoint, mean of ISI-distance, decreased as the synchrony between electrodes within a well increased, indicating an overall increase in synchrony. Figure 3B is a baseline raster plot for one representative well and Figure 3C is the same well 1 hr post treatment with 100 μm bicuculline.
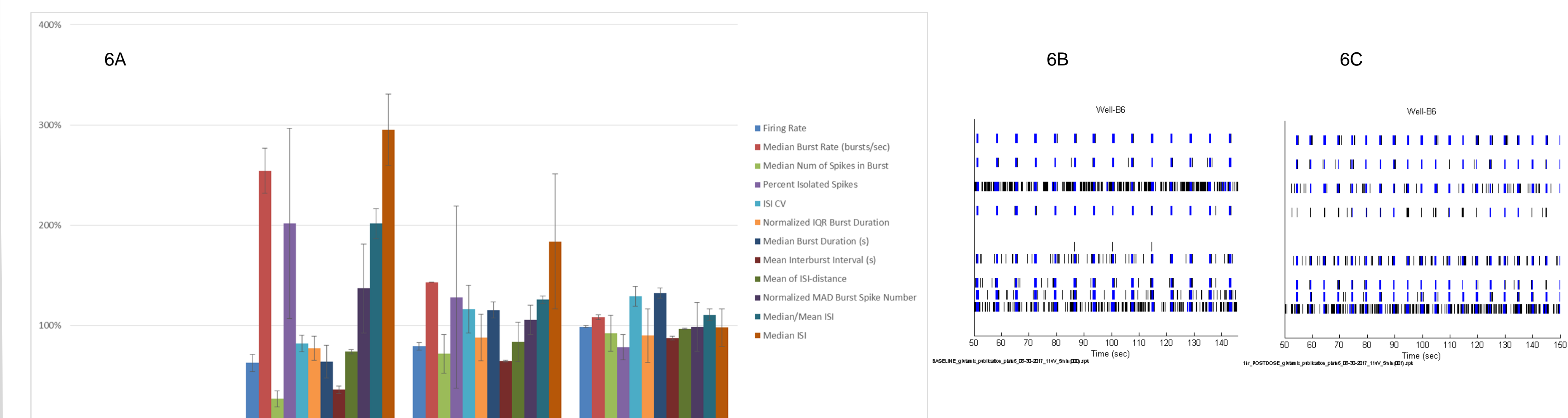
Results: Picrotoxin
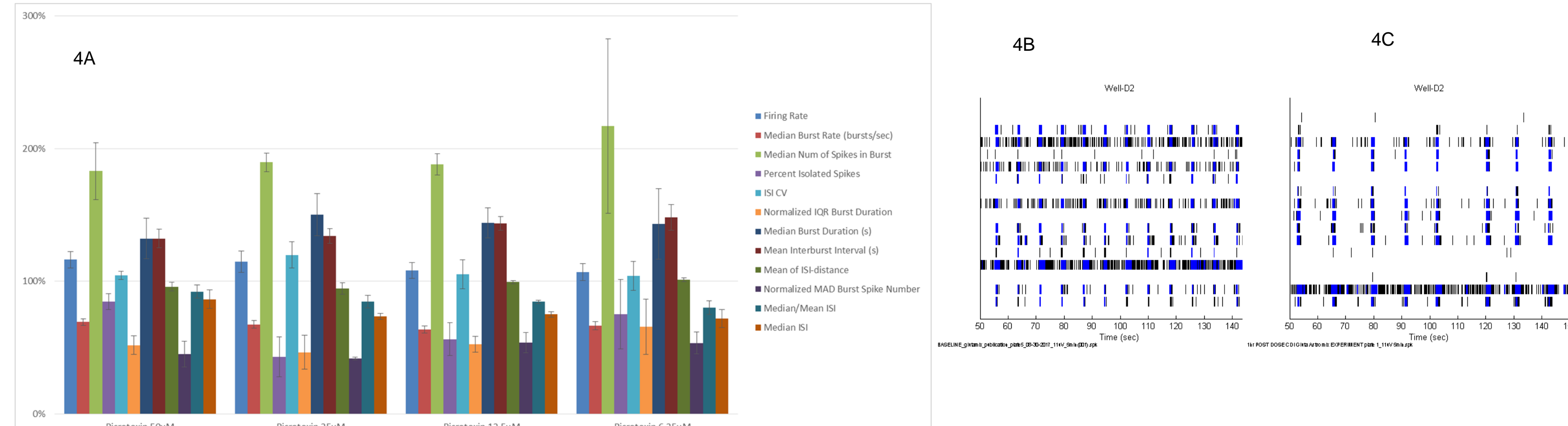
Figures 4A, B, C. Pharmacology results: Picrotoxin. Bar graph (4A) represents fold difference between baseline and 1 hr post dose treatment with picrotoxin at 50, 25, 12.5 and 6.25 μM. Results indicate significant changes in all reported endpoints. There was an overall change in activity with an increase in the spike rate and burst rate for all doses. Burst organization also increased indicated by an increase in the number of spikes in bursts, a decrease in the percent of isolated spikes, a decrease in the normalized IQR burst duration (signifies an increase in burst duration regularity) and an increase in burst duration. The mean interburst interval increased as a result of the decrease in burst rate. Normalized MAD burst spike number (statistical dispersion of spikes in burst), median/mean ISI and median ISI decreased slightly for the top two doses as the synchrony between electrodes within a well increased, indicating an overall increase in synchrony. Figure 4B is a baseline raster plot for one representative well and Figure 4C is the same well 1 hr post treatment with 25 μm picrotoxin.
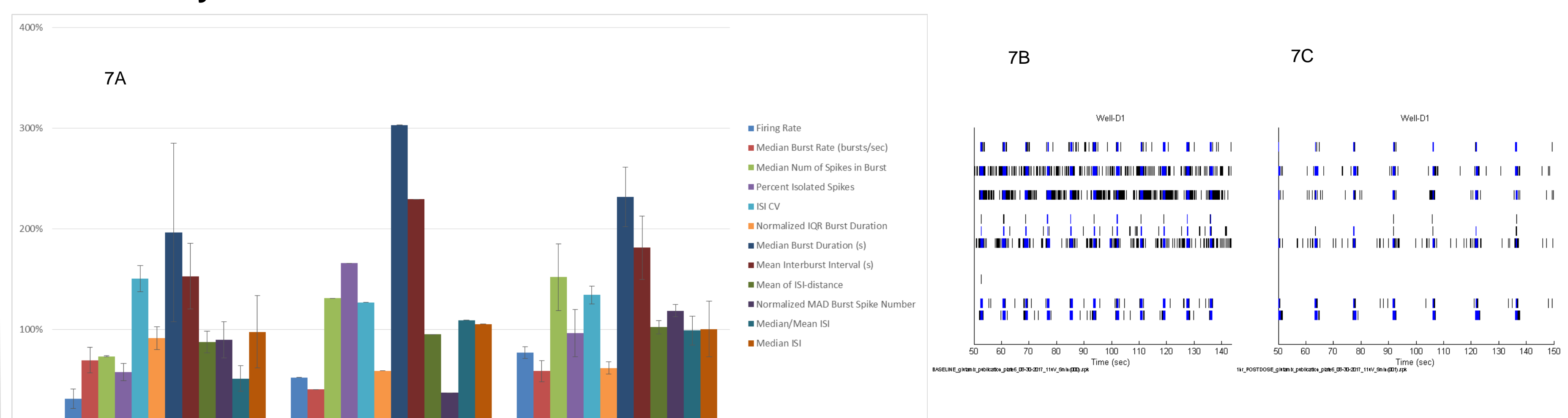
Results: 4-Aminopyridine

Figures 5A, B, C. Pharmacology results: 4-Aminopyridine. Bar graph (5A) represents fold difference between baseline and 1 hr post dose treatment with 4-aminopyridine at 100, 50, 25 and 12.5 μM. Results indicate changes in endpoints related to activity, burst organization and synchrony. The overall change in activity was an increase burst rate for all doses with a slight increase in firing rate. There was an increase in burst organization indicated by a decrease in the percent of isolated spikes, a decrease in the normalized IQR burst duration (signifies an increase in burst duration regularity) and an increase in ISI CV. Burst duration increased at the highest concentration. The mean interburst interval decreased as a result of the increase in burst rate. Normalized MAD burst spike number (statistical dispersion of spikes in burst) decreased, however, the median/mean ISI and median ISI were not significantly effected for most doses. The synchrony endpoint, mean of ISI-distance, decreased slightly for all doses as the synchrony between electrodes within a well increased, indicating an overall increase in synchrony. Figure 5B is a baseline raster plot for one representative well and Figure 5C is the same well 1 hr post treatment with 50 μm 4-aminopyridine.
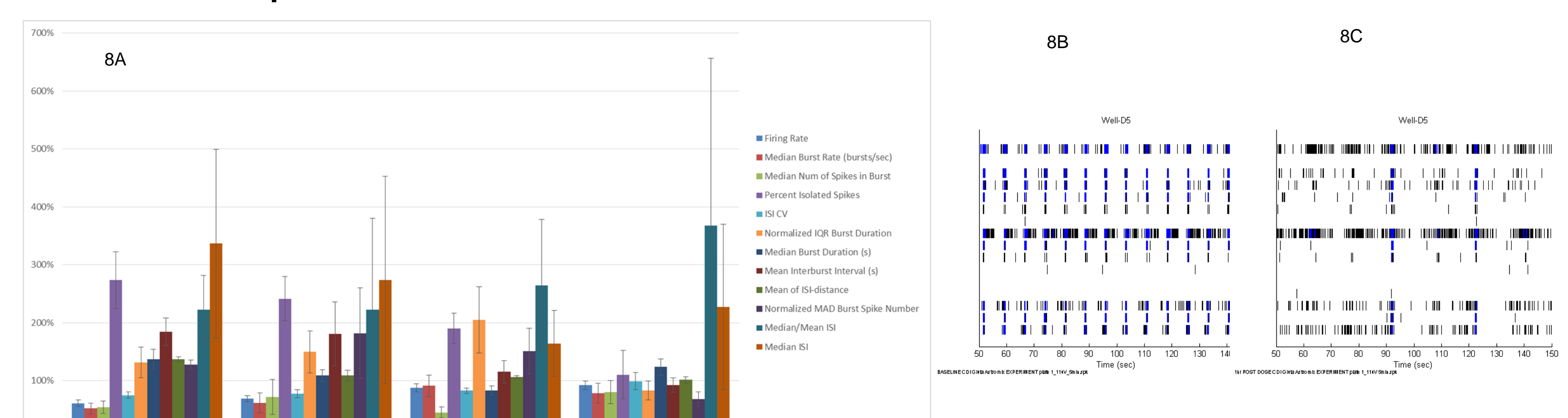
Results: SNC80

Figures 6A, B, C. Pharmacology results: SNC80. Bar graph (6A) represents fold difference between baseline and 1 hr post dose treatment with SNC80 at 20, 10, 5 and 2.5 μM. At 20 μM, SNC80 caused a complete reduction in spike activity. Results for SNC80 at 10 and 5 μM indicate changes in activity, burst organization and synchrony. At 2.5 μM, activity is close to baseline values. The overall change in activity for 10 and 5 μM includes an increase burst rate with a decrease in firing rate. Changes in burst organization included a decrease in the number of spikes in bursts, an increase in isolated spikes, a decrease in the normalized IQR burst duration (signifies an increase in burst duration regularity) and a decrease in burst duration at 10 μM. Normalized MAD burst spike number (statistical dispersion of spikes in burst), the median/mean ISI and median ISI increased at 10 μM. The synchrony endpoint, mean of ISI-distance, decreased slightly for 2 of the doses as the synchrony between electrodes within a well increased, indicating an overall increase in synchrony. Figure 6B is a baseline raster plot for one representative well and Figure 6C is the same well 1 hr post treatment with 10 μm 4-SNC80. Burst organization endpoints were unusual for this compound with some endpoints having contradictory values, therefore additional endpoints will be investigated as well as additional testing with this compound.

Results: Strychnine

Figures 7A, B, C. Pharmacology results: Strychnine. Bar graph (7A) represents fold difference between baseline and 1 hr post dose treatment with strychnine at 30, 15, and 3.75 μM. Results indicate an overall decrease in activity with decreases in both firing rate and burst rate for all doses. Responses for burst characteristic endpoints signify a change in burst organization indicated by changes in the number of spikes in bursts and percent of isolated spikes. An increase in the ISI CV (burstiness) and a decrease in the normalized IQR burst duration (signifies an increase in burst duration regularity) suggest additional changes in burst organization. Burst duration increased for all doses reported. The mean interburst interval increased as a result of the decrease in burst rate. Normalized MAD burst spike number (statistical dispersion of spikes in burst), median/mean ISI and median ISI were not significantly effected. Figure 7B is a baseline raster plot for one representative well and Figure 7C is the same well 1 hr post treatment with 30 μm strychnine. Additional testing with strychnine at different days of maturation are planned, particularly for cultures that have achieved a more synchronous phenotype.

Results: Pilocarpine

Figures 8A, B, C. Pharmacology results: Pilocarpine. Bar graph (8A) represents fold difference between baseline and 1 hr post dose treatment with pilocarpine at 25, 12.5, 6.25 and 3.1 μM. Results indicate changes in endpoints related to activity, burst organization and synchrony. There was an overall decrease in activity with decreases in both firing rate and burst rate for all doses. Responses for burst characteristic endpoints signify a deterioration in burst organization indicated by a decrease in the number of spikes in bursts, and increase in the percent of isolated spikes, a decrease in the ISI CV (burstiness) and an increase in the normalized IQR burst duration (signifies a decrease in burst duration regularity). The mean interburst interval increased as a result of the decrease in burst rate. Normalized MAD burst spike number (statistical dispersion of spikes in burst), median/mean ISI and median ISI increased for most doses, indicating a further breakdown of burst organization. The synchrony endpoint, mean of ISI-distance, increased for the top dose as the synchrony between electrodes within a well decreased, indicating an overall decrease in synchrony. Figure 8B is a baseline raster plot for one representative well and Figure 8C is the same well 1 hr post treatment with 25 μm pilocarpine.

Conclusions

- Early hiPSC derived neuronal models lacked complex burst organization, making MEA-based electrophysiological neurotoxic prediction challenging.
- CDI's iCell GlutaNeurons demonstrate robust and early detectable spike activity with significant increases in burst organization and synchrony over time. Thus forming a complex neural network whose electrophysiological characteristics are easily detected and measured on MEA platforms.
- There is a distinct pattern of change observed as the cells mature, with increases in activity, burst organization and network organization (synchrony). The predictable and observable change in pattern lends itself to testing compounds that could interfere with developmental processes of neural networks.
- The response for GABA$_A$ antagonists, bicuculline and picrotoxin, indicate a robust increase in burst organization with an increase in the spikes that occur in bursts, an increase in the length of the bursts and increases in the regularity of the burst structure and occurrence. Synchrony increases as well, albeit less so when the cells are already at a synchronous level. Additional optimization of the analysis platform and timing of treatment may increase the robustness of this effect.
- The response for 4-aminopyridine, a potassium channel blocker, present quantifiable and reproducible changes in endpoints related to activity, burst organization and synchrony for all of the concentrations tested. Overall, activity, burst organization and network organization increased with treatment.
- The response for SNC80, an opioid receptor agonist, indicate a decrease in spike activity with an increase in burst rate resulting in significant changes in burst organization. Burst organization endpoints were unusual for this compound with some endpoints having contradictory values, therefore additional endpoints will be investigated as well as additional testing with this compound.
- The response for strychnine, a glycine receptor antagonist, indicate an overall decrease in activity for both firing rate and burst rate for all doses. Burst characteristic endpoints also signify changes in burst organization after treatment. Additional testing at different days of maturation are planned, particularly for cultures that have achieved a more synchronous phenotype.
- The response for pilocarpine, a cholinergic and muscarinic receptor agonist, indicate an overall decrease in activity, a deterioration of burst organization and a decrease in synchrony.
- Overall, iCell GlutaNeurons plated with iCell Astrocytes create a robust population of cells that are ideal for evaluating developmental and pharmacological responses when tested on a MEA platform.

References

1. Lei, H. et al, PLoS ONE, (2011), Vol.6, Issue 8
2. Legendy, CR and Salcman, M, J. Neurophysiol., (1985), 53:926-939
3. Kreuz, T, et al, Journal of Neuroscience Methods, (2007) 165:151-161
4. Robinette BL et al, (2011) Front Neuroeng 4; Article 1
5. Novellino A et al, (2011) Front Neuroeng 4; Article 4
6. Johnstone AFM, et al, NeuroToxicology 31 (2010) 331–350